Proceedings of the Eighteenth International Conference on
Civil, Structural and Environmental Engineering Computing
Edited by: P. Iványi, J. Kruis and B.H.V. Topping
Civil-Comp Conferences, Volume 10, Paper 7.3
Civil-Comp Press, Edinburgh, United Kingdom, 2025
ISSN: 2753-3239, doi: 10.4203/ccc.10.7.3

Time-Separated Stochastic Mechanics for Elasto-Viscoplastic Structures

H. Geisler and P. Junker

Institute of Continuum Mechanics, Leibniz University Hannover, Germany

Abstract

Uncertainty quantification allows a more robust estimation of the reliability of structures with random variabilities in material properties. Time-separated Stochastic Mechanics is an efficient and accurate method for uncertainty quantification of materials with microstructure evolution. The method is based on a polynomial surrogate model which separates random from time-dependent behavior. As a result, only a single deterministic simulation has to be performed for each basis function. Analytical expressions for the expectation and standard deviation of quantities of interest, e.g., the stress, can be derived. In this contribution, the Time-separated Stochastic Mechanics is presented for structures with elasto-viscoplastic material behavior. The numerical results show a great agreement with Monte Carlo reference solution on the material point at vastly reduced computational costs. The application on the computation of an artificial dam showcase the potential of the method for the uncertainty quantification of civil structures.

Keywords: time-separated stochastic mechanics, uncertainty quantification, stochastics, elasto-viscoplasticity, finite elements, material model.

1 Introduction

Due to the growing significance of uncertainty quantification in engineering simulations, a variety of methods have been developed. An overview of the most commonly employed methods is presented in Figure 1. In this figure, the methods have been ordered by the computation speed from low to high.

Classically, the Monte Carlo sampling method [1–3] is used for uncertainty quantification due to its simple implementation and vast applicability. In a nutshell, the whole system of equations is simulated for a number of specific realizations of the uncertain parameters. For a high enough number of samples, the expectation, standard deviation and further stochastic quantities can be treated as converged. Undoubtedly, this comes with a very high computational cost as many hundred up to thousands of simulations might be needed to reach a sufficient error level. Quasi-Monte-Carlo methods [4] try to optimize the convergence by using specific sampling rules.

More advanced methods for computationally expensive Finite Element Methods have been developed under the collecting name of Stochastic Finite Element Methods. These are based on a surrogate model which is constructed beforehand. Typically, computations on the surrogate model are much faster compared to the full system of equations. A comparison of the various methods can be found in [5,6]. The stochastic collocation method [7,8] solves the system of equations at a limited number of special evaluation points, often Smolyak points [9]. A polynomial surface is constructed such that the solution is exactly matched at these points. Unfortunately, this method has the recurring issue of instability, see [10].

The polynomial chaos expansion [11, 12] is another well known method. It uses a orthogonal polynomial basis for the surrogate model. A Galerkin projection on this basis of the system of equations is carried out. This enhances the stability compared to the stochastic collocation method. Two main variants of the polynomial chaos expansion are known in literature: a non-intrusive and an intrusive version. The non-intrusive variant uses sampling methods, numerical integration or regression

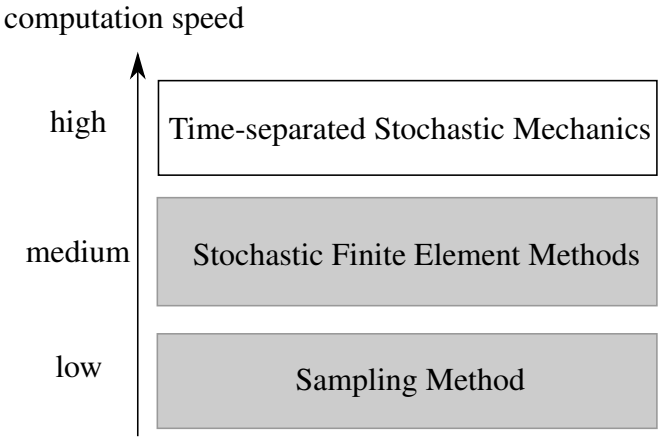

Figure 1: Literature review

approaches, see [13, 14]. Oversampling is required in order to guarantee robustness of the surrogate. The intrusive version, also known as Spectral Stochastic FEM [15, 16], generates a highly coupled system of equations to compute the coefficient of each basis function simultaneously. Clearly, this leads to a rather high computational effort. Furthermore, the Finite Element Solvers solvers have to be adopted.

A method with an even higher computational efficiency is the Time-separated Stochastic Mechanics (TSM) [17, 18]. The polynomial basis exactly matches the derivatives up to a specific order with the parameterized solution. Conceptually, the idea is comparable to a Taylor series. The well known perturbation method [19, 20] can be seen as a special variant of the TSM. In particular, any microstructure development is neglected for the perturbation method. The TSM, in contrast, is specifically designed for microstructure evolution, i.e., for non-linear material laws.

In this contribution, the application of the TSM to civil structures with elasto-viscoplastic behavior is presented. More indepth information on this specific application can be found in [21]. In Section 2, the derivation of the TSM for an elasto-viscoplastic material model is presented. In particular, the derivation of the TSM surrogate and the uncertainty quantification based on the surrogate are explained. In Section 3, numerical experiments are carried out on the material point and for an artificial dam to showcase the applicability of the method. A conclusion is presented in Section 4.

2 Time-separated stochastic mechanics

The behavior of structures is not deterministic. Various effects as microstructural variations, impurities and environmental factors lead to fluctuations of the material properties. In return, this leads to changes of the macroscale behavior. Consequently, the material parameters have to be modeled in dependence of a random variable ξ, i.e., $m(\xi)$. In the following, without loss of generality, we assume that ξ is a zero-centered random variable. The whole set of material parameters might be written as $M = \{m_1(\xi_{1i}, m_2(\xi_{2i})\} = M(\boldsymbol{\Xi})$ with an arbitrary number of random variables. In classical deterministic simulations, only the expectations $\langle m_i \rangle$ are considered. In contrast, the TSM takes the whole randomness of the material parameters into account.

2.1 Surrogate model

In general, the behavior of a structure is governed by the balance of linear momentum

$$\mathcal{L}_{\boldsymbol{u}}(\boldsymbol{u}, \boldsymbol{\alpha}, M(\boldsymbol{\Xi})) := \int_\Omega \delta\boldsymbol{u} \cdot \rho\ddot{\boldsymbol{u}} \,\mathrm{d}V - \int_\Omega \delta\boldsymbol{\varepsilon} \cdot \boldsymbol{\sigma} \,\mathrm{d}V - \int_\Omega \delta\boldsymbol{u} \cdot \boldsymbol{b}^* \,\mathrm{d}V - \int_{\partial\Omega} \delta\boldsymbol{u} \cdot \boldsymbol{t}^* \,\mathrm{d}A = \boldsymbol{0} \tag{1}$$

with the acceleration $\ddot{\boldsymbol{u}}$, stress $\boldsymbol{\sigma}$, body force $\boldsymbol{b}^*$ and traction force $\boldsymbol{t}^*$. The stress $\boldsymbol{\sigma}(\boldsymbol{\varepsilon}, \boldsymbol{\alpha}, M(\boldsymbol{\Xi}))$ depends on the strain $\boldsymbol{\varepsilon} = \nabla^{\mathrm{sym}}\boldsymbol{u}$, some internal variable $\boldsymbol{\alpha}$ and the

uncertain material parameters $M(\boldsymbol{\Xi})$. The internal variable $\boldsymbol{\alpha}$ allows to take the state of the microstructure into account for the stress computation.

As the microstructure develops over time, so does the internal variable. The evolution of the internal variable is described by means of a differential equation

$$\mathcal{L}_{\boldsymbol{\alpha}} = \dot{\boldsymbol{\alpha}} - \boldsymbol{g}(\boldsymbol{\varepsilon}, \boldsymbol{\alpha}, M(\boldsymbol{\Xi})). \tag{2}$$

The evolution equation for elasto-viscoplasticity is given as

$$\mathcal{L}^{\text{evp}}_{\boldsymbol{\alpha}} = \dot{\varepsilon}^{\text{vp}} - \eta^{-1} \left(||\text{dev}(\boldsymbol{\sigma})|| - \sigma^{\text{Y}} \right)_+ \frac{\text{dev}(\boldsymbol{\sigma})}{||\text{dev}(\boldsymbol{\sigma})||} \tag{3}$$

with the internal variable $\boldsymbol{\alpha} = \varepsilon^{\text{vp}}$. The Macaulay brackets are defined as $(x)_+ = \max(0, x)$. The deviatoric part of the stress is calculated as

$$\text{dev}(\boldsymbol{\sigma}) = \boldsymbol{\sigma} - \frac{1}{3} \left(\sigma_1 + \sigma_2 + \sigma_3 \right) \boldsymbol{I} = \mathbb{S} \cdot \boldsymbol{\sigma}.$$

The stress is given as $\boldsymbol{\sigma} = \mathbb{E} \cdot (\boldsymbol{\varepsilon} - \boldsymbol{\varepsilon}^{\text{vp}})$.

In the following, we assume a random elasticity tensor and random yield limit

$$\mathbb{E} = \mathbb{E}^{(0)}(1 + \xi^{\mathbb{E}}) \tag{4}$$

$$\sigma^{\text{Y}} = \sigma^{\text{Y},(0)}(1 + \xi^{\text{Y}}). \tag{5}$$

The random variables $\xi^{\mathbb{E}}, \xi^{\text{Y}}$ are assumed to be multivariate normal with zero mean. It might be noted that other choices of the probability density function can be handled without modification of the TSM.

The main idea of the TSM is the usage of a Taylor series in the random variables as approximation of displacements and internal variable. A linear Taylor series is given as

$$\boldsymbol{u}^{\text{TSM}}(t, \boldsymbol{x}) = \boldsymbol{u}^{(0)}(t, \boldsymbol{x}) + \xi^{\mathbb{E}} \boldsymbol{u}^{\mathbb{E}}(t, \boldsymbol{x}) + \xi^{\text{Y}} \boldsymbol{u}^{\text{Y}}(t, \boldsymbol{x}) \tag{6}$$

$$\boldsymbol{\alpha}^{\text{TSM}}(t, \boldsymbol{x}) = \boldsymbol{\alpha}^{(0)}(t, \boldsymbol{x}) + \xi^{\mathbb{E}} \boldsymbol{\alpha}^{\mathbb{E}}(t, \boldsymbol{x}) + \xi^{\text{Y}} \boldsymbol{\alpha}^{\text{Y}}(t, \boldsymbol{x}) \tag{7}$$

The strain results as $\boldsymbol{\varepsilon}^{\text{TSM}} = \nabla^{\text{sym}} \boldsymbol{u}^{\text{TSM}}$. A Taylor series is a natural choice as the approximation is best near to the expectation. For many probability density functions most of the probability mass is located around the expectation. The extension to a higher-order Taylor series is straight forward. However, it has been noted that for many practical problems, a linear or quadratic Taylor series might suffice, see [19,20]. The Taylor series separates the time-dependent but deterministic terms ($\boldsymbol{u}^{(0)}, \boldsymbol{u}^{\mathbb{E}}, \boldsymbol{u}^{\text{Y}}$ and correspondingly for $\boldsymbol{\alpha}$) from the random but time-independent variables $\xi^{\mathbb{E}}, \xi^{\text{Y}}$.

The Taylor series in Equations (6) and (7) are inserted in the governing equations in (1) and (2). Therefore, the balance of linear momentum for elasto-viscoplasticity in quasi-statics results as

$$\begin{aligned} \mathcal{L}^{\text{evp}}_{\boldsymbol{u}} = \int_\Omega \delta\boldsymbol{\varepsilon}^{(0)} \cdot \left(\mathbb{E}^{(0)}(1 + \xi^{\mathbb{E}}) \right) \cdot \left(\boldsymbol{\varepsilon}^{\text{el},(0)} + \xi^{\mathbb{E}} \boldsymbol{\varepsilon}^{\text{el},\mathbb{E}} + \xi^{\text{Y}} \boldsymbol{\varepsilon}^{\text{el,Y}} \right) \, \text{d}V \\ - \int_\Omega \delta\boldsymbol{u}^{(0)} \cdot \boldsymbol{b}^* \, \text{d}V - \int_{\partial\Omega} \delta\boldsymbol{u}^{(0)} \cdot \boldsymbol{t}^* \, \text{d}A = 0 \quad \forall \delta\boldsymbol{\varepsilon}^{(0)} \quad \forall \delta\boldsymbol{u}^{(0)} \end{aligned} \tag{8}$$

where the relationship $\boldsymbol{\varepsilon}^{\mathrm{el}} = \boldsymbol{\varepsilon} - \boldsymbol{\varepsilon}^{\mathrm{vp}}$ is used.

The zeroth-order terms result by evaluating Equation (8) for $\xi^{\mathbb{E}} = \xi^{\mathrm{Y}} = 0$, i.e., $\mathcal{L}^{\mathrm{evp}}_{\boldsymbol{u}}\big|_{\xi^{\mathbb{E}}=\xi^{\mathrm{Y}}=0}$. Unsurprisingly, the usual deterministic system of equations result as

$$\int_\Omega \delta\boldsymbol{\varepsilon}^{(0)} \cdot \mathbb{E}^{(0)} \cdot \boldsymbol{\varepsilon}^{\mathrm{el},(0)} \,\mathrm{d}V - \int_\Omega \delta\boldsymbol{u}^{(0)} \cdot \boldsymbol{b}^* \,\mathrm{d}V - \int_{\partial\Omega} \boldsymbol{u}^{(0)} \cdot \boldsymbol{t}^* \,\mathrm{d}A = 0, \tag{9}$$

The first-order terms are computed as

$$\frac{\mathrm{d}\mathcal{L}^{\mathrm{evp}}_{\boldsymbol{u}}}{d\xi^{\mathbb{E}}}\Big|_{\xi^{\mathbb{E}}=\xi^{\mathrm{Y}}=0} = \int_\Omega \delta\boldsymbol{\varepsilon}^{(0)} \cdot (\mathbb{E}^{(1)} \cdot \boldsymbol{\varepsilon}^{\mathrm{el},(0)} + \mathbb{E}^{(0)} \cdot \boldsymbol{\varepsilon}^{\mathrm{el},\mathbb{E}}) \,\mathrm{d}V = 0, \tag{10}$$

$$\frac{\mathrm{d}\mathcal{L}^{\mathrm{evp}}_{\boldsymbol{u}}}{d\xi^{\mathrm{Y}}}\Big|_{\xi^{\mathbb{E}}=\xi^{\mathrm{Y}}=0} = \int_\Omega \delta\boldsymbol{\varepsilon}^{(0)} \cdot (\mathbb{E}^{(0)} \cdot \boldsymbol{\varepsilon}^{\mathrm{el},\mathrm{Y}}) \,\mathrm{d}V = 0. \tag{11}$$

Similarly, the TSM terms of the evolution equation are calculated. The zeroth-order term is the usual evolution equation given in (3). The term $\dot{\boldsymbol{\varepsilon}}^{\mathrm{vp},\mathbb{E}}$ is computed by

$$\begin{aligned}
\frac{\mathrm{d}\mathcal{L}^{\mathrm{evp}}_{\boldsymbol{\alpha}}}{d\xi^{\mathbb{E}}}\Big|_{\xi^{\mathbb{E}}=\xi^{\mathrm{Y}}=0} \quad &= \dot{\boldsymbol{\varepsilon}}^{\mathrm{vp},\mathbb{E}}_\gamma(t) \\
&- \frac{1}{\eta}\Bigg(H\left(||\mathrm{dev}(\boldsymbol{\sigma})|| - \sigma^{\mathrm{Y}}\right) \frac{\mathrm{dev}(\boldsymbol{\sigma})_d}{||\mathrm{dev}(\boldsymbol{\sigma})||} \frac{\mathrm{d}}{\mathrm{d}\xi^{\mathbb{E}}}(\mathrm{dev}(\boldsymbol{\sigma})_d) \frac{\mathrm{dev}(\boldsymbol{\sigma})_\gamma}{||\mathrm{dev}(\boldsymbol{\sigma})||} \\
&\quad + \left(||\mathrm{dev}(\boldsymbol{\sigma})|| - \sigma^{\mathrm{Y}}\right)_+ \frac{1}{||\mathrm{dev}(\boldsymbol{\sigma})||} \frac{\mathrm{d}}{\mathrm{d}\xi^{\mathbb{E}}}(\mathrm{dev}(\boldsymbol{\sigma})_\gamma) \\
&\quad + \mathrm{dev}(\boldsymbol{\sigma})_\gamma \frac{\mathrm{d}}{\mathrm{d}\xi^{\mathbb{E}}}\left(||\mathrm{dev}(\boldsymbol{\sigma})||^{-1}\right) \Bigg)\Big|_{\xi^{\mathbb{E}}=\xi^{\mathrm{Y}}=0},
\end{aligned} \tag{12}$$

for each component γ of $\dot{\boldsymbol{\varepsilon}}^{\mathrm{vp},\mathbb{E}}$. No summation is carried out over the index γ. The Heaviside step function is given as $H(x) = \begin{cases} 0, & x < 0 \\ 1, & x \geq 0 \end{cases}$. The further derivatives are found as

$$\frac{\mathrm{d}}{\mathrm{d}\xi^{\mathbb{E}}}(\mathrm{dev}(\boldsymbol{\sigma})_d) = \mathbb{S} \cdot \mathbb{E}^{(1)} \cdot (\boldsymbol{\varepsilon}^{(0)} - \boldsymbol{\varepsilon}^{\mathrm{vp},(0)}) - \mathbb{S} \cdot \mathbb{E}^{(0)} \cdot \boldsymbol{\varepsilon}^{\mathrm{vp},\mathbb{E}} \tag{13}$$

and

$$\frac{\mathrm{d}}{\mathrm{d}\xi^{\mathbb{E}}}(||\mathrm{dev}(\boldsymbol{\sigma})||^{-1}) = -||\mathrm{dev}(\boldsymbol{\sigma})||^{-2} \frac{\mathrm{dev}(\boldsymbol{\sigma})_d}{||\mathrm{dev}(\boldsymbol{\sigma})||} \frac{\mathrm{d}}{\mathrm{d}\xi^{\mathbb{E}}}(\mathrm{dev}(\boldsymbol{\sigma})_d). \tag{14}$$

For the term $\dot{\boldsymbol{\varepsilon}}^{\mathrm{vp},\mathrm{Y}}$, the evolution equation is computed by evaluating

$$\frac{\mathrm{d}\mathcal{L}^{\mathrm{evp}}_{\boldsymbol{\alpha}}}{d\xi^{\mathrm{Y}}}\Big|_{\xi^{\mathbb{E}}=\xi^{\mathrm{Y}}=0} = 0. \tag{15}$$

The evolution equation results as

$$\begin{aligned}
\dot{\boldsymbol{\varepsilon}}^{\mathrm{vp},\mathrm{Y}}_\gamma(t) = \frac{1}{\eta}\Bigg(& H(||\mathrm{dev}(\boldsymbol{\sigma})|| - \sigma^{\mathrm{Y},(0)}) \left(\frac{\mathrm{dev}(\boldsymbol{\sigma})_d}{||\mathrm{dev}(\boldsymbol{\sigma})||} \frac{\mathrm{d}}{\mathrm{d}\xi^{\mathrm{Y}}}(\mathrm{dev}(\sigma)_d) - 1 \right) \frac{\mathrm{dev}(\boldsymbol{\sigma})_\gamma}{||\mathrm{dev}(\boldsymbol{\sigma})||} \\
& + \left(||\mathrm{dev}(\boldsymbol{\sigma})|| - \sigma^{\mathrm{Y},(0)}\right)_+ \frac{\mathrm{d}}{\mathrm{d}\xi^{\mathrm{Y}}}\left(\frac{\mathrm{dev}(\boldsymbol{\sigma})_\gamma}{||\mathrm{dev}(\boldsymbol{\sigma})||} \right) \Bigg)\Big|_{\xi^{\mathbb{E}}=\xi^{\mathrm{Y}}=0}
\end{aligned}$$

with the derivatives

$$\frac{\mathrm{d}}{\mathrm{d}\xi^{\mathrm{Y}}}\Big(\mathrm{dev}(\boldsymbol{\sigma})_d\Big) = -\mathbb{S}\cdot\mathbb{E}^{(0)}\cdot\boldsymbol{\varepsilon}^{\mathrm{vp,Y}}, \tag{16}$$

$$\frac{\mathrm{d}}{\mathrm{d}\xi^{\mathrm{Y}}}\Big(\frac{\mathrm{dev}(\boldsymbol{\sigma})_\gamma}{||\mathrm{dev}(\boldsymbol{\sigma})||}\Big) = \frac{1}{||\mathrm{dev}(\boldsymbol{\sigma})||}\frac{\mathrm{d}}{\mathrm{d}\xi^{\mathrm{Y}}}(\mathrm{dev}(\boldsymbol{\sigma})_\gamma) + \mathrm{dev}(\boldsymbol{\sigma})_\gamma\frac{\mathrm{d}}{\mathrm{d}\xi^{\mathrm{Y}}}(||\mathrm{dev}(\boldsymbol{\sigma})||^{-1}) \tag{17}$$

and

$$\frac{\mathrm{d}}{\mathrm{d}\xi^{\mathrm{Y}}}(||\mathrm{dev}(\boldsymbol{\sigma})||^{-1}) = -||\mathrm{dev}(\boldsymbol{\sigma})||^{-2}\frac{\mathrm{dev}(\boldsymbol{\sigma})_d}{||\mathrm{dev}(\boldsymbol{\sigma})||}\frac{\mathrm{d}}{\mathrm{d}\xi^{\mathrm{Y}}}\Big(\mathrm{dev}(\boldsymbol{\sigma})_d\Big). \tag{18}$$

2.2 Uncertainty quantification

The uncertainty quantification can be carried out as soon as the time-dependent terms have been calculated. This can be done in a post-processing step.

Internal variable The expectation of the internal variable $\boldsymbol{\varepsilon}^{\mathrm{vp}}$ is given as the zeroth-order term

$$\langle\boldsymbol{\varepsilon}^{\mathrm{vp}}\rangle = \boldsymbol{\varepsilon}^{\mathrm{vp},(0)}. \tag{19}$$

The variance of the viscoplastic strain is computed with the relation

$$\mathrm{Var}(\varepsilon_\gamma^{\mathrm{vp}}) = \langle\big(\boldsymbol{\varepsilon}_\gamma^{\mathrm{vp}}\big)^2\rangle - \langle\big(\boldsymbol{\varepsilon}_\gamma^{\mathrm{vp}}\big)\rangle^2 \tag{20}$$

for each component $\boldsymbol{\alpha}$. The second moment $\langle(\varepsilon_\gamma^{\mathrm{vp}}(t))^2\rangle$ results as

$$\langle(\varepsilon_\gamma^{\mathrm{vp}})^2\rangle = (\varepsilon_\gamma^{\mathrm{vp},(0)})^2 + (\varepsilon_\gamma^{\mathrm{vp},\mathbb{E}})^2 + (\varepsilon_\gamma^{\mathrm{vp,Y}}(t))^2 + \varepsilon_\gamma^{\mathrm{vp},\mathbb{E}}\varepsilon_\gamma^{\mathrm{vp,Y}}\langle\xi^{\mathbb{E}}\xi^{\mathrm{Y}}\rangle. \tag{21}$$

A possible correlation of the random variables is accounted for by the last term of Equation (21).

Stress The stress is given as

$$\begin{aligned}\boldsymbol{\sigma} = \mathbb{E}^{(0)}\cdot(\boldsymbol{\varepsilon}^{(0)} - \boldsymbol{\varepsilon}^{\mathrm{vp},(0)}) + \big(\mathbb{E}^{(1)}\cdot(\boldsymbol{\varepsilon}^{(0)} - \boldsymbol{\varepsilon}^{\mathrm{vp},(0)}) + \mathbb{E}^{(0)}\cdot(\boldsymbol{\varepsilon}^{\mathbb{E}} - \boldsymbol{\varepsilon}^{\mathrm{vp},\mathbb{E}})\big)\,\xi^{\mathbb{E}} \\ + \mathbb{E}^{(0)}\cdot(\boldsymbol{\varepsilon}^{\mathrm{Y}} - \boldsymbol{\varepsilon}^{\mathrm{vp,Y}})\xi^{\mathrm{Y}}.\end{aligned} \tag{22}$$

The expectation is found as

$$\langle\boldsymbol{\sigma}\rangle = \mathbb{E}^{(0)}\cdot(\boldsymbol{\varepsilon}^{(0)} - \boldsymbol{\varepsilon}^{\mathrm{vp},(0)}). \tag{23}$$

For the variance, the relation

$$\mathrm{Var}(\sigma_\gamma) = \langle\sigma_\gamma^2\rangle - \langle\sigma_\gamma\rangle^2 \tag{24}$$

involving the second moment is employed again.

The second moment of the stress for each component α is given as

$$\begin{aligned}\langle\sigma_\gamma^2\rangle = \langle\sigma_\gamma\rangle^2 + \Big(\mathbb{E}_{\gamma b}^{(1)}(\varepsilon_b^{(0)} - \varepsilon_b^{\mathrm{vp},(0)}) + \mathbb{E}_{\gamma c}^{(0)}(\varepsilon_c^{\mathbb{E}} - \varepsilon_c^{\mathrm{vp},\mathbb{E}})\Big)^2 + \Big(\mathbb{E}_{\gamma d}^{(0)}(\varepsilon_d^{\mathrm{Y}} - \varepsilon_d^{\mathrm{vp,Y}})\Big)^2 \\ + \Big(\mathbb{E}_{\gamma e}^{(1)}(\varepsilon_e^{(0)} - \varepsilon_e^{\mathrm{vp},(0)}) + \mathbb{E}_{\gamma f}^{(0)}(\varepsilon_f^{\mathbb{E}} - \varepsilon_f^{\mathrm{vp},\mathbb{E}})\Big)\Big(\mathbb{E}_{\gamma g}^{(0)}(\varepsilon_g^{\mathrm{Y}} - \varepsilon_g^{\mathrm{vp,Y}})\Big)\,\langle\xi^{\mathbb{E}},\xi^{\mathrm{Y}}\rangle.\end{aligned} \tag{25}$$

As γ is a fixed component index, no summation is performed over this index.

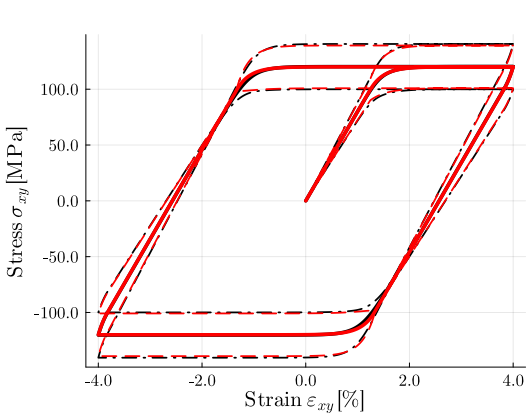

(a) Stress over strain.

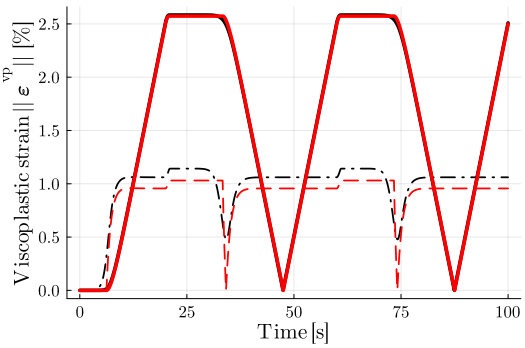

(b) Viscoplastic strain $\boldsymbol{\varepsilon}^{\mathrm{vp}}$ over time. The standard deviation is magnified by a factor of 10.

Figure 2: Material point simulation compared to reference Monte Carlo simulations.

3 Results

First, the TSM approximation is compared on the material point against a Monte Carlo reference solution. At the material point, the strain is given as a deterministic time-proportional function and only the evolution equation is evaluated. The material parameters are chosen as $\langle\lambda\rangle = 12\,\mathrm{GPa}, \langle\mu\rangle = 8\,\mathrm{GPa}, \langle\sigma^{\mathrm{Y}}\rangle = 100\,\mathrm{GPa}$. A rather low viscosity of $\eta = 10\,\mathrm{GPas}$ is chosen to showcase the approximation quality of the TSM even for rapid changes in the behavior. The results are presented in Figure 2. The reference simulation with 1000 Monte Carlo samples is shown in black, the TSM results in red. The expectation is displayed as a solid line, the expectation $\pm$ standard deviation as a dashed line. In the stress-strain diagram in Figure 2a, a hysteresis is well visible. Furthermore, a change in the standard deviation over time is apparent. This highlights the coupling of stochasticity and time. Nevertheless, the TSM approximation is nearly identical to the reference. The same holds for the visco-plastic strains in Figure 2b. Contrary to the expectation that an approximation based on a Taylor series would lead to large deviations near to the yield limit, near to no difference is visible. This is due to the fact that the randomness of the yield limit smooths the transition between elastic and viscoplastic material behavior. The TSM needs approximately the same amount of time as just 20 individual deterministic simulations. A Monte Carlo simulation with this low amount of samples would simply be not converged. Most of the time take the evaluations of Equation (25). For simulations on the structural level the overhead of the evaluations of the analytical equations in Section 2.2 reduces relatively to approximately 10 - 20%, see [21]. The speed-up factor of the TSM compared to the the reference solution is approximately 50.

This speed-up enables uncertainty quantification of civil structures with the Finite Element Method. Here, the boundary value problem of an artificial dam is presented. The dam is discretized by approximately 55.000 quadratic tetrahedron elements. The material parameters are chosen as $\langle\lambda\rangle = 58\,\mathrm{GPa}, \langle\mu\rangle = 39\,\mathrm{GPa}, \langle\sigma^{\mathrm{Y}}\rangle = 100\,\mathrm{MPa}$

and $\eta = 100\,\mathrm{GPah}$. A normal distribution with 10% coefficient of variation is assumed for all random variables. A force due to the water level on the outside of the dam is given. The loading time of the dam is considered negligible compared to the time frame of the microstructure evolution. In Figure 3, the expectation and standard deviation of the stress are presented for two time points. In Figures 3a and 3c, the microstructure still develops and the stress increases whereas in Figures 3b and 3d, the microstructure is nearly stationary. Interestingly, the standard deviation in the middle part of the dam develops contrary to the expectation. The highest standard deviation does not coincide with the highest expectation of the stress. The stress evolution over time of a single element in this area is presented in Figure 4. Here, the solid line indicates the expectation, the dashed lines show the expectation $\pm$ standard deviation. The standard deviation first increases with growing expectation but decreases to a constant value as the change of the expectation diminishes. This highlights the fact, that there is no simple relationship between expectation and standard deviation for structures with microstructure evolution.

4 Conclusion

In this paper, the Time-separated Stochastic Mechanics is presented as an efficient and accurate method for uncertainty quantification of structures with microstructure evolution. Here, the application to an elasto-viscoplastic material behavior is investigated. Numerical examples highlight the great agreement to Monte Carlo reference solutions but also the importance of uncertainty quantification for structures with microstructure evolution.

Acknowledgements

Funded by the European Union (ERC, Gen-TSM, 101124463). Views and opinions expressed are however those of the authors only and do not necessarily reflect those of the European Union or the European Research Council Executive Agency. Neither the European Union nor the granting authority can be held responsible for them.

References

[1] J. E. Hurtado, A. H. Barbat, "Monte Carlo Techniques in Computational Stochastic Mechanics", Archives of Computational Methods in Engineering 5, Nr. 1 (März 1998): 3–29. https://doi.org/10.1007/BF02736747.

[2] R. Ghanem, "Hybrid Stochastic Finite Elements and Generalized Monte Carlo Simulation", Journal of Applied Mechanics 65, Nr. 4 (1. Dezember 1998): 1004–9, https://doi.org/10.1115/1.2791894.

[3] J. S. Liu, Monte Carlo Strategies in Scientific Computing, Springer Series in Statistics, New York, 2004, https://doi.org/10.1007/978-0-387-76371-2.

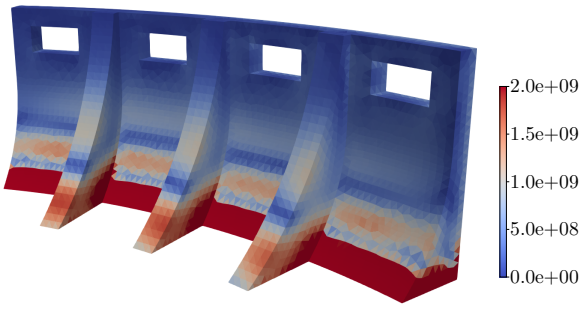

(a) Expectation of the stress during microstructure evolution

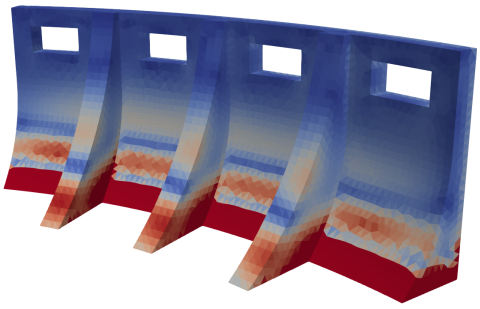

(b) Expectation of the stress for stationary microstructure

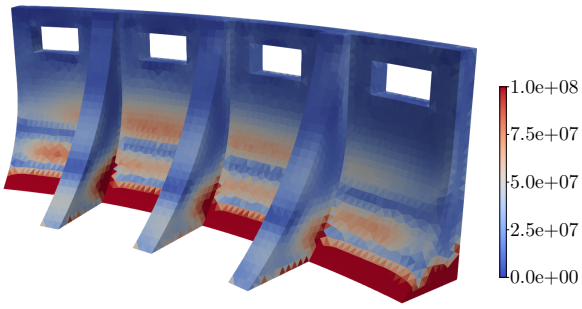

(c) Standard deviation of the stress during microstructure evolution

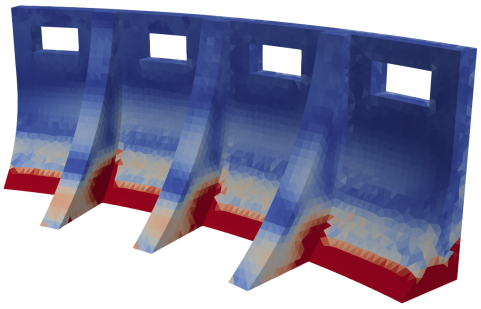

(d) Standard deviation of the stress for stationary microstructure

Figure 3: Boundary value example of an artificial dam.

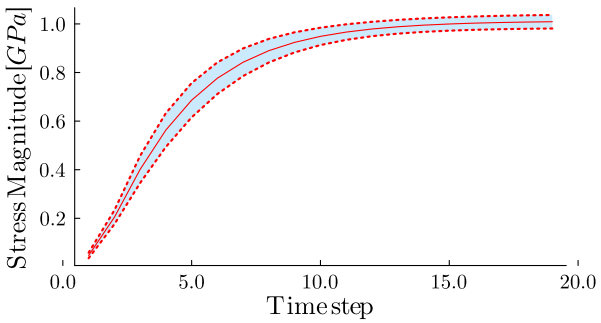

Figure 4: Stress evolution in a specified finite element over time.

[4] L. Plaskota, H. Woźniakowski, Monte Carlo and Quasi-Monte Carlo Methods 2010, Springer Proceedings in Mathematics & Statistics, https://doi.org/10.1007/978-3-642-27440-4.

[5] N. Feng, G. Zhang, K. Khandelwal. "On the Performance Evaluation of Stochastic Finite Elements in Linear and Nonlinear Problems", Computers & Structures 243 (Januar 2021): 106408, https://doi.org/10.1016/j.compstruc.2020.106408.

[6] R. V. Field, M. Grigoriu, J.M. Emery, "On the Efficacy of Stochastic Collocation, Stochastic Galerkin, and Stochastic Reduced Order Models for Solving Stochastic Problems", Probabilistic Engineering Mechanics 41 (Juli 2015): 60–72, https://doi.org/10.1016/j.probengmech.2015.05.002.

[7] D. Xiu, "Stochastic Collocation Methods: A Survey", in Handbook of Uncertainty Quantification, R. Ghanem, D. Higdon, H. Owhadi, 1–18. Cham: Springer International Publishing, 2016, https://doi.org/10.1007/978-3-319-11259-626-1.

[8] M. Gunzburger Max, C. G. Webster, G. Zhang, "Sparse Collocation Methods for Stochastic Interpolation and Quadrature", in Handbook of Uncertainty Quantification, R. Ghanem, D. Higdon, H. Owhadi, 717–62, Springer International Publishing, 2017, https://doi.org/10.1007/978-3-319-12385-1.

[9] D. Xiu, J. S. Hesthaven, "High-Order Collocation Methods for Differential Equations with Random Inputs", SIAM Journal on Scientific Computing 27, Nr. 3 (Januar 2005): 1118–39, https://doi.org/10.1137/040615201.

[10] M. Dannert, F. Bensel, A. Fau, R. Fleury, U. Nackenhorst, "Investigations on the Restrictions of Stochastic Collocation Methods for High Dimensional and Nonlinear Engineering Applications", Probabilistic Engineering Mechanics 69 (Juli 2022), https://doi.org/10.1016/j.probengmech.2022.103299.

[11] D. Xiu, G. Karniadakis, "The Wiener-Askey Polynomial Chaos for Stochastic Differential Equations", SIAM Journal on Scientific Computing 24, Nr. 2 (Januar 2002): 619–44, https://doi.org/10.1137/S1064827501387826.

[12] B. Sudret, "Polynomial Chaos Expansions and Stochastic Finite Element Methods", in Risk and Reliability in Geotechnical Engineering, K. Phoon, J. Ching, 265–300, CRC Press, 2014.

[13] H. Matthies, A. Keese, “Galerkin Methods for Linear and Nonlinear Elliptic Stochastic Partial Differential Equations“, Computer Methods in Applied Mechanics and Engineering 194, Nr. 12–16 (April 2005): 1295–1331, https://doi.org/10.1016/j.cma.2004.05.027.

[14] M. Hadigol, A. Doostan, “Least Squares Polynomial Chaos Expansion: A Review of Sampling Strategies“, Computer Methods in Applied Mechanics and Engineering 332 (April 2018): 382–407, https://doi.org/10.1016/j.cma.2017.12.019.

[15] R. Ghanem, , P. Spanos, Stochastic Finite Elements: A Spectral Approach, New York Berlin Heidelberg: Springer, 1991.

[16] B. Debusschere, “Intrusive Polynomial Chaos Methods for Forward Uncertainty Propagation“, in Handbook of Uncertainty Quantification, R. Ghanem, D. Higdon, H. Owhadi, 617–36, Springer International Publishing, 2017, https://doi.org/10.1007/978-3-319-12385-119.

[17] H. Geisler, P. Junker, “Time-Separated Stochastic Mechanics for the Simulation of Viscoelastic Structures with Local Random Material Fluctuations“, Computer Methods in Applied Mechanics and Engineering 407 (März 2023): 115916, https://doi.org/10.1016/j.cma.2023.115916.

[18] H. Geisler, C. Erdogan, J. Nagel, P. Junker, “A New Paradigm for the Efficient Inclusion of Stochasticity in Engineering Simulations: Time-Separated Stochastic Mechanics“, Computational Mechanics 75, Nr. 1 (Januar 2025): 211–35, https://doi.org/10.1007/s00466-024-02500-5.

[19] W. Liu, T. Belytschko, A. Mani. “Random Field Finite Elements“, International Journal for Numerical Methods in Engineering 23, Nr. 10 (Oktober 1986): 1831–45, https://doi.org/10.1002/nme.1620231004.

[20] M. Kleiber, T.D. Hien, The stochastic finite element method: basic perturbation technique and computer implementation. Wiley, 1992.

[21] H. Geisler, P. Junker, “Efficient and Accurate Uncertainty Quantification in Engineering Simulations Using Time-Separated Stochastic Mechanics“, Archive of Applied Mechanics 94, Nr. 9 (September 2024): 2603–17, https://doi.org/10.1007/s00419-024-02590-w.